Theoretical Study of the Adsorption of Bisulfate on Small Gold Clusters

Marc D. Legault*

Department of Physics, University of Puerto Rico at Bayamón, 170 Road 174, Parque Industrial Minillas, Bayamón, PR 00959

Daniel E. Bacelo

Department of Sciences and Technology, Universidad Metropolitana, P.O. Box 21150, San Juan, PR 00927-1150

Received: March 6, 2002; In Final Form: May 28, 2002

The results of density functional theory energy calculations of bisulfate adsorbed to gold atom clusters are presented and discussed. The gold atom clusters are used to model a gold(111) surface. These calculations involve the Becke three-parameter functional to approximate the exchange energy and the Lee, Yang, and Parr approximation to include the electronic correlation contribution. The structure and stability of the bisulfate ion at different adsorption sites on the gold surface are examined. The bisulfate in its tripod orientation is found to be the most stable configuration due to the direct interaction of each oxygen of the tripod with a gold atom of the surface. The binding of the bisulfate is predominantly electrostatic and is strongly dependent on the local charge of the gold up to second-nearest neighbors from the adsorption site. Additionally, the bisulfate prefers the face-centered cubic 3-fold hollow adsorption site directly above a hollow in the second layer and a gold atom in the third layer.

1. Introduction

Aqueous sulfuric acid is one of the most important electrolytes in use in the chemical industries. There are numerous studies regarding the role of its dissociated ions, bisulfate or sulfate, in the adsorption of metallic ions on noble metal substrates.[1,2] Which particular species bisulfate or sulfate, is adsorbed on noble metal substrates is still hotly debated in electrochemical circles.[3−6] In this article the notation (bi)sulfate will refer to either species. The study of the adsorption of (bi)sulfate on metallic surfaces is a complex problem and is pertinent technologically to battery chemistry, dissolution of metals in acids, electroplating, and metallic monolayer formation. The problem of anion adsorption in an electrochemical interface has received much experimental attention due to the anion's role in altering the structure and charge distribution at the interface.[7−9] The interpretations of these experimental results are controversial, although it is generally accepted that in the presence of water, the (bi)sulfate can form a commensurate $\sqrt{3} \times \sqrt{7}$ monolayer[10,11] and, under ultrahigh vacuum conditions, a commensurate $\sqrt{3} \times \sqrt{3}$ (bi)sulfate monolayer on a gold(111) surface.[12] Clear-cut conclusions regarding the adsorption site and bisulfate geometry have not yet been reached. It is believed that the (bi)sulfate anion is adsorbed at a 3-fold hollow site via three oxygen atoms. Theoretical quantum mechanical studies can help in the interpretation of electrochemical *in situ* experiments such as surface X-ray, infrared spectra, and scanning tunneling microscopy. However, at the present time, there are few highly accurate electronic structure studies of the interaction between bisulfate or sulfate and a gold surface.[13−15] Patrito et al.[13] have studied extensively the nature of the sulfate−Ag(111) surface bond. They also discuss some preliminary results of the sulfate−Au(111) bonding and provide some comparisons with the Ag(111) case. Their calculations have been done at the second-order Møller−Plesset (MP2) level of theory with very large metallic clusters (28−64 atoms) approximating the surface. Each metal atom of the primary chemisorption site (4−6 atoms) is treated using the Huzinaga relativistic effective core potentials (RECPs) for the core electrons and 11 valence electrons whereas the rest of the atoms of the cluster are treated as 1-electron atoms. Their study found that the sulfate binds to the gold-(111) surface in a 3-fold hollow via three oxygen atoms pointed toward the second-nearest gold atoms. The most stable binding energy for sulfate onto a neutral bulk-terminated gold(111) surface was found to be 143.9 kcal/mol. A comparison between the adsorption of sulfate, bisulfate, and sulfuric acid on different silver surfaces is reported in the work of Olivera et al.[14] Like their previous work, they have used MP2 calculations on large clusters and have used 4−6 11-electron silver atoms at the primary chemisorption site. They find the interesting result that the binding energy of H_2SO_4, HSO_4^-, and SO_4^{2-} to silver is linear with the square of their effective charge on the surface. Xu et al. have investigated, using a first-principles pseudopotential plane wave method, the coadsorption of copper and sulfate on a gold(111) surface.[15] They also report a calculation of sulfate on a bulk-terminated Au(111) surface where the most stable configuration obtained is the one where the sulfate is adsorbed to a 3-fold hollow via three oxygens pointed toward the first-nearest gold atoms.

In this study we will use density functional theory (DFT) approximations to obtain realistic prediction of the interaction between the bisulfate and gold(111) surface. The cluster approach is used to approximate the gold surface. The most stable orientation and most favorable adsorption site of the adsorbed bisulfate onto a gold surface with (111) orientation are determined with the use of relatively large basis sets describing 60 core and 19 valence electrons for the gold atoms. The different adsorption sites considered in this study are the

10.1021/jp0257303 CCC: $22.00
Published on Web 09/04/2002

top (directly over a gold atom), fcc and hcp 3-fold hollow (hollow formed by three gold atoms), and bridge (between two gold atoms) adsorption sites. Additionally, the effect of total charge of the bisulfate−gold clusters on the binding energy was investigated. Changing the total charge of the cluster mimics the effect of changing the potential of the gold surface that occurs, for example, during a voltammetric study of the adsorption of bisulfate onto that surface. Voltammetry can give explicit information of the energetics and dynamics of the adsorption process, it does not yield explicit information of the surface structure. The theoretical structures obtained in this study can complement voltammetric studies to deepen our understanding of the (bi)sulfate adsorption process.

2. Computational Methods

Partial structure optimizations were performed for many possible configurations of the $[Au_nHSO_4]^m$ system, where the number of gold atoms n was varied as $3 \leq n \leq 13$ and the charge m was varied as $-2 \leq m \leq +2$. The Gaussian 98 software package[16] was used to compute the energies at the DFT level[17] using the three-parameter Becke hybrid[18] with the Lee, Yang, and Parr correlation functional (B3-LYP).[19] DFT methods offer savings in computational time over the post Hartree−Fock second-order Møller−Plesset perturbation theory[20] (HF-MP2) calculations. DFT approximations have been applied successfully in studies of metal and molecular clusters.[21,22] Progress in recent years in developing nonlocal corrections to the local density approximation has produced DFT methods able to reliably predict geometries of a complex system like those treated here.[18,19,23] Due to the difficult electronic convergence of the system, the quadratic convergence criteria at the self-consistent field level was applied in all the optimizations. As the gold atoms are quite large, the 60 inner-shell core electrons were treated via effective core potentials (ECP).[24] The ECPs were chosen to incorporate relativistic effects, such as mass−velocity and Darwing effects, and as such, they describe the relativistic contraction of the s and p shells. The average relativistic effective potentials (AREP), and the associated (5s5p4d)/[4s3p3d] basis set of Ross et al.,[25] were employed to describe the 60 core and 19 valence electrons of the gold atom. This basis set includes the 5s, 5p, 5d, 6s, and 6p subshells in the valence space. The calculations were performed using the 6-311+G** basis sets for the hydrogen, oxygen, and sulfur atoms.

The structure optimizations of the bisulfate molecule onto a fixed gold cluster were performed under the single constraint of limiting the sulfur to move along a normal through the adsorption site on the gold cluster, as shown in Figure 1. The other atoms of the bisulfate molecule had all degrees of freedom. Each structure optimization was performed with several different starting configurations to minimize trapping within the same potential well. The Au−Au distance and the Au−Au−Au angles for all gold clusters were constrained to the experimental bulk values.[26] The Au−Au distance was set to 2.88 Å with a Au−Au−Au angle of 60°. The binding energy of adsorption for a particular configuration is calculated using

$$E_{\text{bind}} = E^{\text{opt}}_{\text{HSO}_4^-} + E^{\text{sp}}_{\text{Au}_n{}^q} - E^{\text{opt}}_{\text{Au}_n\text{HSO}_4{}^{q-1}} \qquad (1)$$

where $E^{\text{opt}}_{\text{HSO}_4^-}$ and $E^{\text{opt}}_{\text{Au}_n\text{HSO}_4{}^{q-1}}$ are the geometrically optimized energy for the bisulfate and bisulfate−gold cluster, respectively, and $E^{\text{sp}}_{\text{Au}_n{}^q}$ is the single point energy of the gold cluster. All species are calculated at the DFT B3-LYP level.

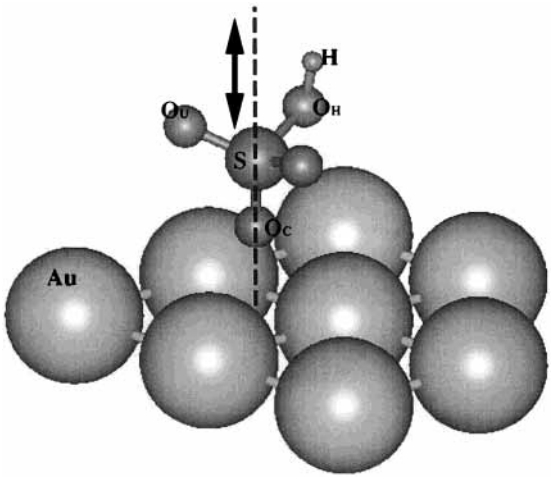

Figure 1. Schematic representation of the single constraint of the structure optimizations.

3. Results and Discussion

3.1. Configurational Stability. During voltammetric scans involving the sulfuric acid electrolyte on single-crystal surfaces of noble metals such as, gold, platinum, silver etc., it is believed that (bi)sulfate forms ordered monolayers when the surface is positively charged. The primary purpose of this study is to determine which bisulfate configuration is most stable on a gold surface with (111) surface orientation. Gold clusters reflecting the symmetry of the adsorption site and bisulfate configuration were chosen to eliminate possible artificial strain on the bisulfate, which would manifest itself in a higher binding energy. The total charge of the gold−bisulfate system was set to zero to approximate a positively charged gold surface at an electrochemical interface. The binding energies (and optimized geometries) of the adsorption of bisulfate to the 3-fold hollow with C_{3v} symmetry in the 1-oxygen (1-H) or 3-oxygen down (3-H) configuration of the following gold clusters were determined: Au_3, Au_6, and Au_{12}. The binding energies (and optimized geometries) of the adsorption of bisulfate on top of a gold atom with C_{3v} symmetry, in the 1-oxygen (1-T) or 3-oxygen down (3-T) configuration of the following gold clusters were determined: Au_4 and Au_7. And, finally, the binding energy (and optimized geometry) of the adsorption of bisulfate on the bridge site with C_{2v} symmetry, in the 2-oxygen down (2-B) configuration of the Au_4 gold cluster was determined. Figure 2 shows the adsorption sites and symmetry of the above clusters.

Although the use of these particular gold clusters eliminated symmetry artifacts from the calculations, it proved difficult to determine the most stable configuration, as cluster size ultimately influenced the binding energy to a much greater degree than possible symmetry effects. See Table 1 for the binding energies for these symmetric clusters. Let us point out two significant observations on the binding energies from Table 1. First, although the trend in stability exhibited here does in fact correspond to the trend found for different configurations on gold clusters of larger size, the results were found inconclusive due to the fact that for configurations of similar symmetry, the binding energy changed dramatically as the cluster size increased. Second, as the cluster size is increased, the binding energies are found to decrease. An explanation of this trend is related to local electrostatic effects occasioned by the preset charge and the small size of the cluster. This will be discussed fully in a later section.

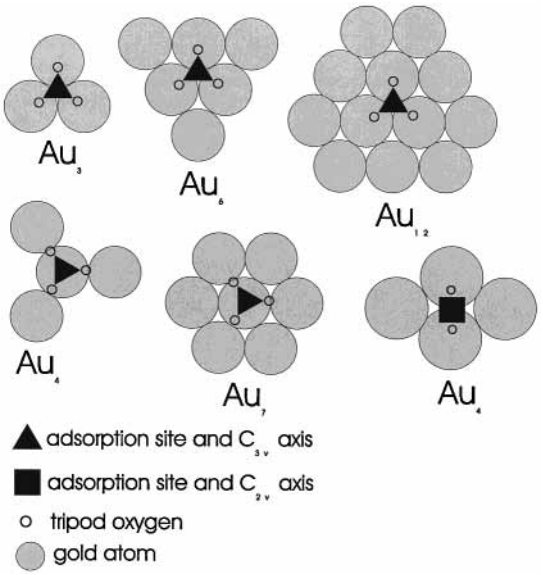

Figure 2. Top view of the adsorption sites and symmetry of gold clusters.

The Au_8 cluster was chosen to investigate the configurational stability of bisulfate on gold. It is believed that this cluster is sufficiently large that, given our large basis set and computational resources, the study becomes feasible and conclusive. Figure 3 shows the optimized structures found for bisulfate adsorbed to the Au_8 cluster with a total charge of zero.

Table 2 gives the binding energies for various optimized configurations of bisulfate onto the Au_8 cluster representing the Au(111) surface for different preset charges. For the system consisting of the negative bisulfate adsorbing to a neutral gold surface ($q = -1$), in decreasing order of stability, the following was found: 3-oxygen down hollow adsorption site, 2-oxygen down bridge, 3-oxygen down top, 1-oxygen down hollow, and 1-oxygen down top. These results suggest that the single most important factor affecting stability is the number of oxygen−gold interactions. Shared interactions between one oxygen atom to many gold atoms are stronger than one direct oxygen−gold interaction but weaker than two direct oxygen−gold interactions. The 3-H bisulfate configuration maximizes the number of such strong direct oxygen−gold interactions and evidently has the highest binding energy of 20.22 kcal/mol. Although it is known that the DFT applicability to negative ions is questionable,[27] large molecular anions with low net charge show minimal ill effects due to the reduction of self-repulsion by the large spatial extent of the charge distribution.[28] Patrito et al. also show that the 3-H sulfate on Au(111) is the most stable.[13,14] However, their sulfate molecule is rotated 60° from our optimized structure obtained for bisulfate, such that the oxygens are directly above bridge sites and pointing toward second-nearest neighbor gold atoms. There are possibly many reasons for the observed difference. First, two different systems are being compared: bisulfate and sulfate. This reason is unlikely as there is evidence that oxyanions on metal surfaces give the same adsorbate.[29,30] Basis set superposition error (BSSE) may be a possible explanation as this error is quite large, as evidenced by the BSSE calculated for the 3-H bisulfate configuration on neutral gold. However, our study failed to find a minimum in the potential energy surface for the bridge-oriented bisulfate−gold supermolecule. A most probable reason for the difference is the fact that the gold RECPs used in this study consisted of 60 core and 19 valence electrons, as opposed to the RECPs used in the work of Patrito et al. Our study is consistent with the periodic pseudopotential study of Xu and Wang,[15] which involves the adsorption of sulfate on gold(111). Xu and Wang also show that the sulfate is found in the 3-H configurations with the oxygens of the sulfate tripod in the top orientation (toward 1st-nearest gold) rather than the bridge orientation (toward second-nearest gold).

3.2. Total Charge Effects. As is well evident in Table 2, the binding energy is very sensitive to the total charge of the bisulfate−gold system. This suggests that the binding energy of the bisulfate monolayer on a positively charged single-crystal noble metal surface is mostly electrostatic in origin. In our previous work on the statistical mechanics of the underpotential deposition of copper on gold in the presence of sulfuric acid, we have obtained adsorption isotherms for the bisulfate anion.[31,32] These isotherms show that at high positive potentials (with respect to the standard hydrogen electrode) the bisulfate has a large coverage, and as one decreases the potential of the gold surface, the bisulfate desorbs.

In the work cited above, the binding energy was phenomenologically related to charge and potential and is found to be completely in agreement with the findings of this present study. The binding energies and the partial charge of bisulfate determined by a Mulliken population analysis, for two clusters, as a function of total charge are presented in Table 3. Figure 4 suggests a linear relationship between binding energy and partial charge on gold. The gold partial charge was also obtained using the Mulliken population analysis and the sum of both partial charges equals the total charge of the cluster. This graph demonstrates that the binding energy of bisulfate onto gold is proportional to the gold charge, which is linearly related to the electric field or electric potential of the surface. Extrapolation of the graph toward the more negative side suggests that there is a potential (or charge) where the bisulfate no longer binds to the surface and consequently desorbs from the surface. Deviations from linearity imply that the binding also involves an electron overlap character. The results of Table 3 also show that the bisulfate anion transfers a charge equal to −1 minus its partial charge to the gold surface during adsorption. Figure 5 shows that the binding energy is proportional to the charge transferred to the gold surface. This behavior suggests that during charge transfer the system is stabilized by a quantity related to the work function of the metal per electron. This correlation is also found between sulfur oxides on transition metals.[33]

Significant parameters defining the geometry of the bisulfate−gold system (Au_8HSO_4) as a function of charge are tabulated in Table 4. As the parameters from Table 4 indicate, when the gold surface charge increases, the electrostatic attraction to the negative bisulfate increases. This results in the bisulfate binding closer to the surface as is, for example, evidenced by the gold−sulfur distance of the 3-H cluster changing from 3.54 to 3.37 Å and the bond between the coordinated oxygen(s) and the gold atom(s) shortening from 2.76 to 2.48 Å. The coordinated oxygen−sulfur bond elongates, for example, from 1.52 to 1.55 Å for the 1-H cluster, due to the increased electronic density between coordinated oxygen and gold. Consequently, in the case of the 1-H cluster, a shortening of the sulfur−uncoordinated oxygen bond occurs due to bond conservation[34] from 1.469 to 1.461 Å. The anticorrelation between intermolecular distances and intramolecular bond lengths is also typical for systems with weak interactions such as van der Waals or H-bond interactions.[22,35] As the bisulfate approaches nearer to the 3-fold hollow in the 3-H position, the angle between the O_C-S-O_H increases from 103.7° to 105.3° due to the electrostatic attraction between

TABLE 1: Binding Energies (kcal/mol) of Selected Symmetric Bisulfate−Gold Clusters with Total Charge of Zero

3-H		2-B		3-T		1-H		1-T	
Au_3HSO_4	118.6	Au_4HSO_4	106.0	Au_4HSO_4	106.5	Au_3HSO_4	99.8	Au_4HSO_4	91.0
Au_6HSO_4	102.8	N. A.		Au_7HSO_4	87.6	Au_6HSO_4	95.3	Au_7HSO_4	80.3
$Au_{12}HSO_4$	90.9	N. A.		N. A.		$Au_{12}HSO_4$	82.8	N.A.	

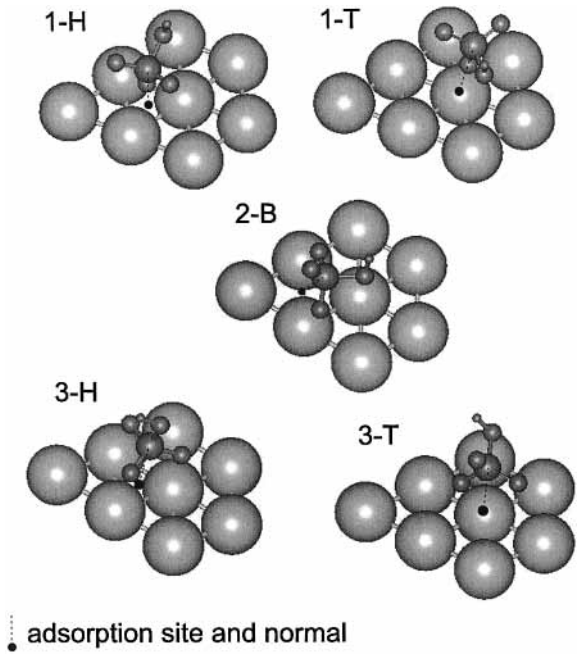

Figure 3. Optimized structures of $Au_8(HSO_4)$ configurations with total charge of zero.

TABLE 2: Binding Energies (kcal/mol) of the Au_8HSO_4 Cluster with Different Preset Charges

$[Au_8HSO_4]^q$	3-H	2-B	3-T	1-H	1-T
$q = -1$	20.2	20.0	16.7	14.4	12.9
$q = 0$	95.1	91.2	89.1	84.0	81.4
$q = +1$	175.3	168.6	170.6	162.1	157.6

TABLE 3: Binding Energies (kcal/mol) of Two Clusters with Preset Charges from −2 to +2

cluster	parameter	−2	−1	0	+1	+2
Au_3HSO_4, 3-H	bind. energy	no binding	14.1	118.6	266.7	442.8
	HSO_4^- charge	N.A.	−0.683	−0.460	−0.175	0.089
Au_6HSO_4, 3-H	bind. energy	no binding	15.7	102.8	201.3	303.3
	HSO_4^- charge	N.A.	−0.674	−0.456	−0.288	−0.147

gold and oxygen atoms. This creates a more closed structure due to the tendency of the oxygen atoms to move directly above a corresponding gold atom. The opposite effect is seen for the 1-H configuration: as the bisulfate approaches nearer to the surface, the O_C-S-O_H decreases from 101.7° to 97.8°, opening the oxygen tripod. This is due, in this case, to the shortening of the distance and consequent increase of the interactions between O_C and the gold atoms. The inverse relationship between the number of bonds and relaxation is exhibited for the 1-T and 3-H configurations where, in both cases, the coordinated oxygens interact directly with a gold atom. For example, for $q = -1$ the $Au-O_C$ distance for the 3-H (with three bonds) is 2.7620 Å and the $Au-O_C$ distance for the 1-T (with one bond) is 2.4933 Å. This clearly suggests the tendency for the bisulfate molecule to maximize the interactions with the gold surface, forcing in the case of the 1-T with only one direct interaction between the Au and O, to move closer to the surface, resulting in the shortest Au−O distance of all configurations.

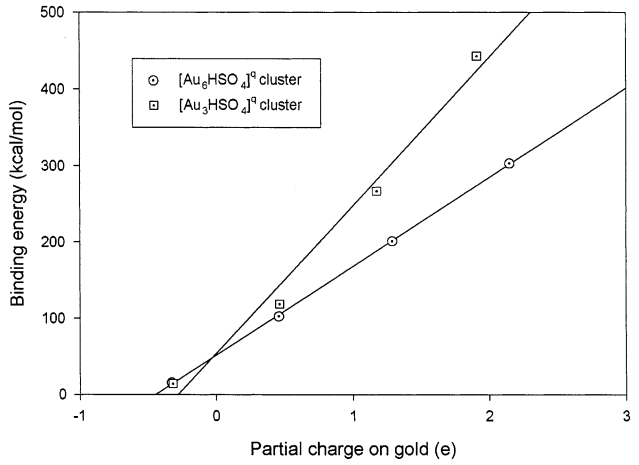

Figure 4. Relationship between the binding energy and partial charge on the gold atoms.

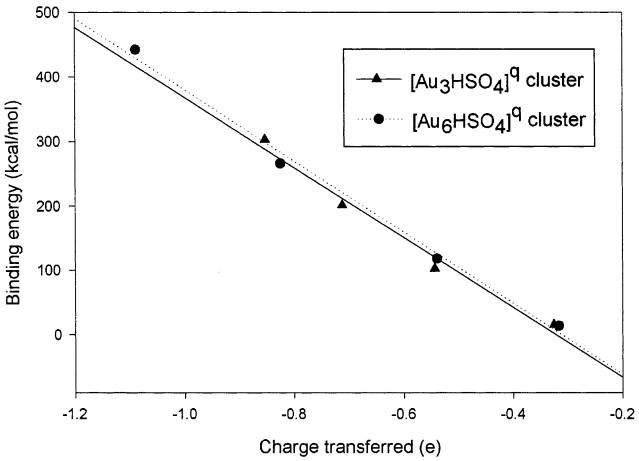

Figure 5. Relationship between the binding energy and charge transferred to the gold cluster.

3.3. One-Layer Cluster Size Effects. For clusters with total charge of −1 it is found that the binding energy increases as the system size increases. However, in the charged system ($q \geq 0$), the binding energy decreases as the cluster size increases. Table 5 gives the binding energies and significant distances between the bisulfate (3-H) and the gold surface for the 1-layer gold clusters Au_3, Au_6, and Au_{12} for charges −1 and 0. A Mulliken charge population analysis shows that the coordinated gold atoms become very positively charged due to charge transfer from the gold atoms to the bisulfate molecule. As expected, the oxygen atoms of the bisulfate are found to be negatively charged. The outer gold atoms in each cluster are also found to be negatively charged. For the Au_6 cluster these outer atoms consists of the three first-nearest neighbor atoms to the coordinated gold atoms, and for the Au_{12} cluster these consist of the six second-nearest neighbor atoms from the hollow adsorption site. This is an artifact due to the inability of the small 1-layer gold cluster to efficiently distribute the charge, such that positive charge is concentrated around the coordinated gold atoms that directly interact with oxygen atoms. The negative ring of charge found on the outer gold neighbors

TABLE 4: Significant Geometrical Parameters for $[Au_8(SO_4H)]^q$

cluster		parameter									
structure	charge	Au−O_C[a,b]	Au−O_H[a,b]	Au−O_U[a,b]	S−O_C[b]	S−O_U[a,b]	S−O_H[a]	Au−S[a]	O_H−H	O_C−S−O_U[a]	O_C−S−O_H[a]
1-H	−1	2.798	4.248	4.405	1.517	1.468	1.682	4.118	0.974	113.1	101.7
	0	2.663	4.201	4.400	1.524	1.467	1.671	3.969	0.975	113.0	98.7
	1	2.564	3.891	4.145	1.548	1.461	1.655	3.875	0.977	110.9	97.8
1-T	−1	2.493	4.678	4.760	1.498	1.472	1.689	3.992	0.973	113.4	103.3
	0	2.446	4.416	4.707	1.497	1.471	1.667	3.944	0.975	113.1	100.1
	1	2.363	4.339	4.714	1.510	1.467	1.650	3.873	0.977	111.7	99.6
2-B	−1	2.586	4.244	4.808	1.498	1.462	1.673	3.693	0.974	115.3	103.8
	0	2.491	4.082	4.688	1.499	1.464	1.663	3.601	0.975	114.7	102.6
	1	2.412	4.034	4.598	1.508	1.458	1.647	3.547	0.976	113.9	102.0
3-H	−1	2.762	5.075	N.A.	1.477	N.A.	1.676	3.538	0.974	N.A.	103.7
	0	2.629	4.913	N.A.	1.482	N.A.	1.649	3.436	0.975	N.A.	104.4
	1	2.476	4.783	N.A.	1.492	N.A.	1.626	3.372	0.977	N.A.	105.2
3-T	−1	2.548	3.997	4.925	1.479	1.465	1.681	3.609	0.975	115.5	104.3
	0	2.524	3.860	4.687	1.475	1.466	1.668	3.360	0.974	115.2	103.4
	1	2.417	3.941	4.502	1.481	1.459	1.646	3.250	0.976	115.1	103.7

[a] Average parameter. [b] Lower parameter. O_C and O_U refer to the coordinated and uncoordinated oxygen. O_H refers to the hydrogen-bonded oxygen. Distances are in angstroms; angles, in degrees. All optimizations were performed with 6-311+G(d,p) basis sets.

TABLE 5: Binding Energies (kcal/mol) and Separation of the Bisulfate (Å) to the Gold Surface Function of Cluster Size and Charge

structure	BE	Au−O_C	Au−S	structure	BE	Au−O_C	Au−S
$[Au_3HSO_4]^{-1}$	14.1	2.897	3.619	$[Au_3HSO_4]^0$	118.6	2.524	3.336
$[Au_6HSO_4]^{-1}$	15.7	2.831	3.580	$[Au_6HSO_4]^0$	102.8	2.635	3.423
$[Au_{12}HSO_4]^{-1}$	19.7	2.820	3.575	$[Au_{12}HSO_4]^0$	90.9	2.648	3.439

weakens the attraction between the coordinated oxygens and the gold surface. Consequently, the bisulfate separates further from the surface with an associated lowering of the binding energy. We can conclude that cluster size is fundamental to how well the cluster approximates a real surface. These results also show the importance of local charge distribution (or potential) on the optimized structure, geometry, and stability of adsorbates. To our knowledge, these charge (or potential) effects have not been investigated in previous studies.

3.4. Multilayer Cluster Size Effects. A gold crystal with (111) surface orientation forms a structure with alternating layers ABCABCABC..., due to its face-centered cubic (fcc) lattice.[26] This generates two distinct 3-fold hollow sites on the surface, the hexagonal close-packed (hcp) 3-fold hollow and the fcc 3-fold hollow. The hcp 3-fold hollow is directly above an atom in the second layer and a hollow in the third layer. The fcc 3-fold hollow is directly above another hollow in the second layer and an atom in the third layer. The binding energies of two symmetric bisulfate−gold clusters ($Au_{10}HSO_4$ and $Au_{13}HSO_4$), with total charge of −1, simulating these two different adsorption sites were obtained. The total charge of −1 was used to resolve the small electronic differences between the two adsorption sites. The electrostatic contributions to the binding energy for a total charge greater than −1 are 1 order of magnitude greater than the quantum mechanical contribution. The $Au_{10}HSO_4$ cluster consists 6, 3, and 1 gold atoms in the first, second, and third layer, respectively, and features the adsorption of bisulfate on the fcc 3-fold hollow site. The $Au_{13}HSO_4$ cluster consists of 6 and 7 gold atoms in the first and second layer and features the adsorption of bisulfate on the hcp 3-fold hollow site. The hollow in the third layer is represented by the absence of a gold atom. See Figure 6 for a top view of these two gold clusters. The binding energy of the hcp hollow configuration was determined at 35.98 kcal/mol and that of the fcc hollow configuration at 38.37 kcal/mol. Although the hcp hollow configuration is a larger cluster it nevertheless has a smaller binding energy than the fcc hollow configuration. This is a strong indication that the fcc hollow configuration is favored.

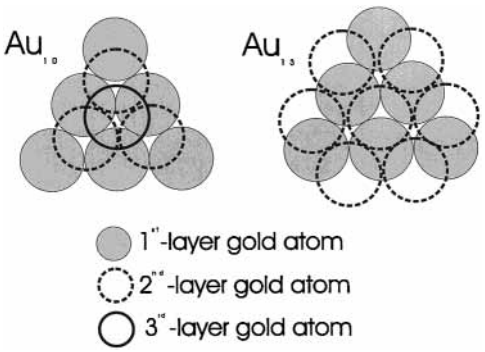

Figure 6. Top view of the multilayer clusters.

4. Conclusions

All significant optimized configurations for the bisulfate ion adsorbed to clusters consisting of 3−13 gold atoms were found. It was determined that the most stable structure is the one where the sulfur is in the fcc 3-fold hollow and where three oxygens are pointed downward and pointed toward the three first-nearest gold atoms. This most stable structure maximizes the number of oxygen−gold interactions. The highest binding energy obtained for this configuration with a total charge of −1 was found to be 38.37 kcal/mol. The difference in the binding energy between the fcc and hcp 3-fold hollow adsorption was found to be 2.39 kcal/mol. It is found that the total charge on the system strongly affects the binding energy and geometrical parameters of the bisulfate. As the binding increases, the bisulfate in the three oxygen down configuration becomes nearer to the surface with a consequent closing of the oxygen tripod. The interaction energy is principally electrostatic, as is suggested by a linear dependence between binding energy and partial charge (or electric potential) of the gold surface. The binding energy is also found to be linear with the amount of charge transferred from the bisulfate to the gold atoms.

Acknowledgment. We acknowledge the computational time provided from the High Performance Computing Facility of the University of Puerto Rico. M.L. acknowledges release time awarded by the Academic Investigation Committee of the University of Puerto Rico in Bayamón. D.B. acknowledges the support of the NSF-MIE program at the Universidad Metropolitana.

References and Notes

(1) Lipkowski, J.; Ross, P. N. *Adsorption of Molecules at Metal Electrodes*; VCH: New York, 1992; Chapter 4.
(2) Lipkowski, J.; Ross, P. N. *Structure of Electrified Interfaces*; VCH: New York, 1993; Chapter 2.
(3) Shi, Z.; Lipkowski, J.; Gamboa, M.; Zelenay, P.; Wieckowski, A. *J. Electroanal. Chem.* **1994**, *366*, 317.
(4) Ataka, K.; Osawa, M. *Langmuir* **1998**, *14*, 951.
(5) Kim, Y.-G.; Soriaga, J. B.; Vigh, G.; Soriaga, M. P. *J. Colloid Interface Sci.* **2000**, *227*, 505.
(6) Kolics, A.; Wieckowski, A. *J. Phys. Chem. B* **2001**, *105*, 2588.
(7) Zelenay, P.; Rice, L. M.; Wieckowski, A. *Surf. Sci.* **1991**, *256*, 253.
(8) Shi, Z.; Lipkowski, J. *J. Electroanal. Chem.* **1994**, *365*, 303.
(9) Shi, Z.; Wu, S.; Lipkowski, J. *Electrochem. Acta* **1995**, *40*, 9.
(10) Magnussen, O. M.; Hageböck, J.; Hotlos, J.; Behm, R. J. *J. Chem. Soc. Faraday Discuss.* **1992**, *94*, 329.
(11) Edens, G. J.; Gao, X.; Weaver, M. J. *J. Electroanal. Chem.* **1994**, *375*, 357.
(12) Mrozek, P.; Han, M.; Sung, Y.-E.; Wieckowski, A. *Surf. Sci.* **1994**, *319*, 21.
(13) Patrito, E. M.; Olivera, P. P.; Sellers, H. *Surf. Sci.* **1997**, *380*, 264.
(14) Olivera, P. P.; Patrito, E. M.; Sellers, H. *Surf. Sci.* **1998**, *418*, 376.
(15) Xu, J. G.; Wang, X. W. *Surf. Sci.* **1998**, *408*, 317.
(16) Frisch, M. J.; Trucks, G. W.; Schlegel, H. B.; Scuseria, G. E.; Robb, M. A.; Cheeseman, J. R.; Zakrzewski, V. G.; Montgomery, J. A., Jr.; Stratmann, R. E.; Burant, J. C.; Dapprich, S.; Millam, J. M.; Daniels, A. D.; Kudin, K. N.; Strain, M. C.; Farkas, O.; Tomasi, J.; Barone, V.; Cossi, M.; Cammi, R.; Mennucci, B.; Pomelli, C.; Adamo, C.; Clifford, S.; Ochterski, J.; Petersson, G. A.; Ayala, P. Y.; Cui, Q.; Morokuma, K.; Malick, D. K.; Rabuck, A. D.; Raghavachari, K.; Foresman, J. B.; Cioslowski, J.; Ortiz, J. V.; Stefanov, B. B.; Liu, G.; Liashenko, A.; Piskorz, P.; Komaromi, I.; Gomperts, R.; Martin, R. L.; Fox, D. J.; Keith, T.; Al-Laham, M. A.; Peng, C. Y.; Nanayakkara, A.; Gonzalez, C.; Challacombe, M.; Gill, P. M. W.; Johnson, B. G.; Chen, W.; Wong, M. W.; Andres, J. L.; Head-Gordon, M.; Replogle, E. S.; Pople, J. A. *Gaussian 98*, revision A.7; Gaussian, Inc.: Pittsburgh, PA, 1998.
(17) Parr, R.; Yang, W. *Density-Functional Theory of Atoms and Molecules*; Oxford University Press: New York, 1989.
(18) Becke, A. D. *J. Chem. Phys.* **1988**, *88*, 1053.
(19) Lee, C.; Yang, W.; Parr, R. G. *Phys. Rev. B* **1988**, *37*, 785.
(20) Møller, C.; Plesset, M. S. *Phys. Rev.* **1934**, *46*, 618.
(21) (a) Ziegler, T. *Chem. Rev.* **1991**, *91*, 651. (b) Mlynarski, P.; Salahub, D. R. *J. Chem. Phys.* **1991**, *95*, 6050.
(22) (a) Bacelo, D. E.; Ishikawa, Y. *Chem. Phys. Lett.* **2000**, *319*, 679. (b) Bacelo, D. E.; Binning, R. C., Jr; Ishikawa, Y. *J. Chem. Phys. A* 1**999**, *103*, 4631. (c) Bacelo, D. E.; Ishikawa, Y. *J. Mol. Struct. (TEOCHEM)* **1998**, *425*, 87.
(23) Perdew, J. P.; Wang, *Y. Phys. Rev. B* **1992**, *45*, 13244.
(24) (a) Kahn, L. R.; Goddard, W. A., III. *J. Chem. Phys.* **1972**, *56*, 2685. (b) Kahn, L. R.; Hay, P. J.; Cowan, R. D. *J. Chem. Phys.* **1978**, *68*, 3059.
(25) Ross, R. B.; Powers, J. M.; Atashroo, T.; Ermler, W. C.; LaJohn, L. A.; Christiansen, P. A. *J. Chem. Phys.* **1990**, *93*, 6840.
(26) Kittel, C. *Introduction to Solid State Physics*, 6th ed.; John Wiley: New York, 1986; Chapter 1.
(27) Sellers, H.; Patrito, E. M.; Olivera, P. P. *Surf. Sci.* **1996**, *352*, 222.
(28) Markovits, A.; García-Hernández, M.; Ricart, J. M.; Illas, F. *J. Phys. Chem. B* **1999**, *103*, 509.
(29) Galbraith, J. M.; Schaefer, J. M., III. *J. Chem. Phys.* **1996**, *105*, 862.
(30) Rösch, N.; Trickey, S. B. *J. Chem. Phys.* **1997**, *106*, 8940.
(31) Legault, M. D.; Blum, L.; Huckaby, D. A. *J. Electroanal. Chem.* **1996**, *409*, 79.
(32) Blum, L.; Legault, M. D.; Huckaby, D. A. *Interfacial Electrochemistry*: *Theory*, *Experiment*, *and Applications*; Marcel Dekker: New York, 1999; Chapter 2.
(33) Sellers, H.; Shustorovich, E. *Surf. Sci.* **1996**, *346*, 322.
(34) Shustorovich, E. *Adv. Catal.* **1990**, *37*, 101.
(35) Schütz, M.; Klopper, W.; LüThi, H. P.; Leutwyler, S. *J. Chem. Phys.* **1995**, *103*, 6114.